J. M. Siddaway, S. V. Petelina, D. J. Karoly, A. R. Klekociuk, and R. J. Dargaville

Evolution of Antarctic ozone in September-December predicted by CCMVal-2 model simulations for the 21st century

Atmospheric Chemistry and Physics, 2013; 13(8):4413-4427

Atmos. Chem. Phys., 13, 4413–4427, 2013
www.atmos-chem-phys.net/13/4413/2013/
doi:10.5194/acp-13-4413-2013

Atmospheric Chemistry and Physics Open Access

Evolution of Antarctic ozone in September–December predicted by CCMVal-2 model simulations for the 21st century

J. M. Siddaway[1], S. V. Petelina[1], D. J. Karoly[2], A. R. Klekociuk[3], and R. J. Dargaville[2]

[1]Department of Physics, La Trobe University, Bundoora VIC 3086, Australia
[2]School of Earth Sciences, University of Melbourne, Melbourne VIC 3010, Australia
[3]CPC Program, Australian Antarctic Division, Kingston TAS 7050, Australia

Correspondence to: J. M. Siddaway (j.siddaway@latrobe.edu.au)

Received: 15 June 2012 – Published in Atmos. Chem. Phys. Discuss.: 1 August 2012
Revised: 5 April 2013 – Accepted: 8 April 2013 – Published: 29 April 2013

Abstract. Chemistry-Climate Model Validation phase 2 (CCMVal-2) model simulations are used to analyze Antarctic ozone increases in 2000–2100 during local spring and early summer, both vertically integrated and at several pressure levels in the lower stratosphere. Multi-model median trends of monthly zonal mean total ozone column (TOC), ozone volume mixing ratio (VMR), wind speed and temperature poleward of 60° S are investigated. Median values are used to account for large variability in models, and the associated uncertainty is calculated using a bootstrapping technique. According to the trend derived from the twelve CCMVal-2 models selected, Antarctic TOC will not return to a 1965 baseline, an average of 1960–1969 values, by the end of the 21st century in September–November, but will return in ∼2080 in December. The speed of December ozone depletion before 2000 was slower compared to spring months, and thus the decadal rate of December TOC increase after 2000 is also slower. Projected trends in December ozone VMR at 20–100 hPa show a much slower rate of ozone recovery, particularly at 50–70 hPa, than for spring months. Trends in temperature and winds at 20–150 hPa are also analyzed in order to attribute the projected slow increase of December ozone and to investigate future changes in the Antarctic atmosphere in general, including some aspects of the polar vortex breakup.

1 Introduction

It has been over 25 yr since the first measurements of significant stratospheric ozone depletion over Antarctica (Farman et al., 1985) was linked with an increase in anthropogenic halogen loading (e.g., Solomon et al., 1986). That discovery contributed to the establishment of the Montreal Protocol in 1987 to regulate global emissions of ozone depleting substances (ODS), such as chlorofluorocarbons (CFCs), containing Cl_y and Br_y compounds. A peak in total combined chlorine surface abundances was observed in mid-1990s, and these are now either zero or in decline (WMO, 2007). Such decline is often measured by Equivalent Effective Stratospheric Chlorine (EESC) levels. EESC combines Cl_y and Br_y into a single quantity that leads to ozone depletion. Following on from the decline in surface emissions, global mean concentrations of EESC are now decreasing as well (e.g. Newman et al., 2007). Successful outcomes of global agreements, such as the Montreal Protocol, provide an example that regulations of anthropogenic emissions entering the atmosphere are achievable and beneficial. Establishing if the ozone layer over Antarctica has begun to recover and how long the recovery to pre-ozone hole levels might take is important, as this information may inform future policy on halogen compound production. The subject of when the ozone recovers and at what rates has many other important implications, such as possible effects of this process on surface climate in Antarctica (Perlwitz et al., 2008) and over the Southern Hemisphere in general (Son et al., 2010). Antarctic ozone increase may also affect lower stratospheric circulation and mean age of air in the Northern Hemisphere (Deushi and Shibata, 2011).

One available method to investigate how a reduction in atmospheric halogen loading to natural "background" levels will lead to stratospheric ozone recovery in the near future is to analyse simulations from state-of-the-art coupled chemistry-climate models (CCMs). Such models are widely

used to predict the future behavior of stratospheric ozone in response to different forcings (e.g Eyring et al., 2007). They provide simulations of various atmospheric parameters in three-dimensional space coupled with fully interactive stratospheric ozone chemistry. The degree of ozone recovery can also be affected by other changes in the atmospheric composition, such as current and future increase in concentrations of greenhouse gases (GHG). These will affect ozone levels and complicate the attribution of direct ozone recovery from decreased halogens (Eyring et al., 2010b).

Numerous results on regional and global ozone and climate applications have already been derived from CCMVal-2 model simulations (e.g. Eyring et al., 2010a). CCMVal-2 model studies that consider future projections of total ozone column (TOC) often use annual globally averaged TOC over extra-polar latitudes and mean October monthly zonal mean TOC values to represent Antarctic spring ozone trends (e.g. Austin et al., 2010a). Different from other studies, the present analysis focuses on unique aspects of future Antarctic ozone increase, in particular monthly rates and speeds of TOC increase in austral spring and early summer (September–December).

Several studies have investigated the predicted relationship between stratospheric chlorine loading and TOC from CCMVal-2 model output (e.g. Eyring et al., 2010a; Oman et al., 2010). Austin et al. (2010a) considered the decline and recovery of Antarctic October multi-model mean TOC using CCMVal-2 future simulations with respect to both a 1960 and a 1980 baseline. A direct comparison with October mean Cl_y at 50 hPa and TOC found a very similar trend between the two when a 1980 baseline is selected with both quantities returning to baseline values in ∼2055. When a 1960 baseline is chosen, the October mean Cl_y at 50 hPa does not return to baseline before the end of the century, and the October TOC returns shortly before 2100. Oman et al. (2010) found a similar result, relative to a 1960 baseline, when considering the partial column ozone at 500–20 hPa. These model studies indicate that EESC levels will greatly influence the return pattern of increasing ozone subsequent to peak depletion. The effect of increasing GHG emissions on climate change will also affect the ozone return date to a 1960 value, especially towards the end of the 21st century. Here we consider projections of Antarctic ozone increase due to both decreasing ODSs and climate change, rather than a relationship between stratospheric chlorine levels and ozone.

Ozone recovery is usually expressed in terms of an ozone increase related to a removal of anthropogenically produced ODSs (WMO, 2007). Ozone return date refers to ozone increase to a pre-defined level (or reference year such as 1980 or 1960) prior to the depletion period. As a result, return of stratospheric ozone to a certain pre-defined value and a full ozone recovery can be reached at different times (e.g. Waugh et al., 2009; Eyring et al., 2010a).

Newman et al. (2006) found that full ozone recovery to 1980 levels, based purely on future ODS levels, will occur around 2068. Oman et al. (2010) considered evolution of partial columns in the 21st century and found that for the lower stratosphere (integrated over the 500–20 hPa range), peak spring ozone (October) returned to 1960 levels in ∼2090. That study included a similar selection of REF-B2 model simulations as we used. They also calculated a multi-model trend in EESC at 50 hPa and found a decrease to ∼85 % of 1960 levels by 2100 (see Fig. 10 in Oman et al., 2010), therefore attributing much of the trend in the lower stratosphere October ozone to the trend in EESC. Eyring et al. (2010b) considered different GHG sensitivity simulations for CCMVal-2 models and found that the SRES A2 scenario (more GHGs by 2100 than in the A1B scenario) resulted in a decrease of ozone in the lower stratosphere during the 21st century. The B1 scenario (less GHGs by 2100 than in the A1B scenario) leads to an increase in ozone by the end of the century. However, the overall differences resulting from different GHG scenarios were minor. Alternatively, Waugh et al. (2009) found that when the effect of climate change alone was considered, there were minimal decadal-scale variations in Antarctic spring ozone from 1960 until 2100. In that study, mean October ozone VMR at 50 hPa, as well as October TOC, were predicted to recover to a 1960 value by 2100 due to the combined forcing effect of GHG and ODS. Using a single CCM, Perlwitz et al. (2008) found that with chlorine fixed at 1960 values and using the A1B GHG scenario, October ozone at 70 hPa did not fluctuate significantly in 2000–2099. However, it could also be that the 1960 levels of chlorine were not sufficient to exert enough influence on ozone, compared to the amount that was observed in the mid-1990s.

The aim of this study is to analyze Antarctic ozone evolution and return dates with respect to a historical baseline of 1960–1969 values using the output from several CCMs. This baseline level is an averaged value of TOC that has not yet been significantly perturbed by ODS. There are differing opinions on what time period to select as a baseline for ozone recovery estimations. It is common to use the 1980 value (e.g WMO, 2007), which is an average of 1975–1984 values, as the Antarctic ozone depletion was relatively small at that time. On the other hand, Newman et al. (2007) reported that EESC have been increasing rapidly before 1985, and thus the 1975–1984 baseline period may not correspond to the unperturbed ozone state. In this work, a baseline derived from a mean of 1960–1969 values is used, hereafter referred to as a 1965 baseline, as stratospheric ozone was not yet significantly affected by anthropogenic halogen emissions at that time (e.g. Farman et al., 1985). This is further supported by the Jones and Shanklin (1995) results, who found that a decline in the ozone concentration during October became apparent in the early 1970s, while Hofmann et al. (1997) looked at 10 yr of ozonesonde data from the South Pole and found that there was no ozone depletion before 1970.

In this work, we investigate the projected evolution of Antarctic ozone using monthly mean simulated TOC data

in September–December zonally averaged poleward of 60° S and analyze variations of TOC with respect to the corresponding pre-ozone hole baseline levels. While many studies that focus on the ozone hole employ multi-model mean TOC values, we use multi-model median TOC and ozone mixing volume ratio (VMR). As the spread in individual model outputs can be large, especially for ozone concentrations at various pressure levels, using the median function gives an advantage of assigning a lower weight to the most deviating data. To quantify the uncertainty associated with the multi-model median values, namely a 95 % confidence level, a bootstrapping technique was used. In order to generate the statistical uncertainty, a subsample of individual model median values was randomly sampled with replacement 1000 times to produce a normal distribution of medians. From this distribution, a confidence limit was calculated.

Previous CCMVal-2 model studies (e.g. Eyring et al., 2010a; Austin et al., 2010a) analysed a multi-model mean with associated uncertainties using a Time-Series Additive Model (TSAM) as described in Chapter 9 of SPARC CCM-Val (2010) If so, please add the reference to the reference list. If not, it would be clearer to change the name to CCM-Val (2010) and in Scinocca et al. (2010). The advantage of using this technique is that model simulations of various time lengths can still be used to produce a robust mean trend over the full reference period of 1960–2100. In this study, only the model simulations that provided output over the entire study period were selected. It was also found that using a 1960 value as a baseline in the TSAM analysis resulted in a larger inter-model spread in TOC, compared to a 1980 baseline value (SPARC CCMVal, 2010). In this study, investigating multi-model median TOC and ozone VMR from model time series of equal lengths relative to a 1965 baseline could be considered advantageous as a lower weight is assigned to individual models that deviate mostly from the median.

In addition to TOC, we also analysed effects of a projected ozone increase in the 21st century on the polar vortex by assessing monthly temperature and zonal mean zonal wind variations over the September–December period. Different from this work, previous CCMVal-2 model studies usually considered seasonally averaged values of temperature and zonal wind (e.g. SPARC CCMVal, 2010; Son et al., 2010) rather than on a month-by-month basis.

2 Model simulations

Stratospheric Processes and their Role in Climate Project (SPARC) Chemistry-Climate Model Validation phase 2 (CCMVal-2) Report (SPARC CCMVal, 2010) is a coordinated model intercomparison that included results from up to 17 CCMS, with some models providing a wider variety of simulations than others. 16 of these models offer future reference simulations (REF-B2) for the CCMVal-2 activity to project ozone trends towards the end of the 21st century (Eyring et al., 2010a). REF-B2 simulations are transient simulations from 1960 to 2100 that contain time series of surface hydrocarbon halogens based on the adjusted World Meteorological Organisation (WMO) A1 scenario (WMO, 2007) and surface GHG concentrations based on the Special Report on Emissions Scenario A1B (IPCC, 2000). These REF-B2 simulations of the future atmospheric state essentially include anthropogenic forcings only, such as varying GHG surface concentrations and prescribed halogen emissions, with natural forcings due to solar variability and volcanic activity being excluded. This is different from REF-B1 simulations that include both natural and anthropogenic forcings (Eyring et al., 2007).

We note that Austin et al. (2010b) analysed metrics of the Antarctic ozone hole, such as minimum ozone and ozone mass deficit, from CCMVal-2 model output by comparing both REF-B1 and REF-B2 simulations. Such an approach is not considered in this study, as for our purposes it is preferential to work with a continuous and homogenous dataset and these two sets of simulations have different sources of uncertainty in their model integrations. REF-B1 simulations address internal uncertainties within each model with external forcings being based on observations, whereas REF-B2 simulations have external uncertainty associated with biases from climate models that provide prescribed forcings. Of all models used in this study, a quasi-biennial oscillation (QBO) signal is only included in those models that internally simulate QBO, namely MRI, UMSLIMCAT and the UKUCMA (SPARC CCMVAL, 2010). All models except CMAM have prescribed sea surface temperature (SST) and sea ice cover (SIC) from coupled ocean model simulations (Eyring et al., 2010a; Morgenstern et al., 2010). A more detailed description of each model formulation is given by SPARC CCM-VAL (2010) and by Morgenstern et al. (2010) and will not be repeated here.

Monthly mean TOC values were available for 14 models that participated in the REF-B2 simulations. Two out of these 14 models were excluded from the present analysis: GEOSCCM provided a future simulation only from 2000, UMUKCA-METO only provided data until 2083. Monthly mean ozone VMR were available for 11 models out of the 12 selected for TOC values. However, all 12 models were used for stratospheric temperatures and zonal mean wind metrics. There were variations in the ensemble size for each model: most models provided a single ensemble member, with the exception of MRI (2 ensemble members) and the CMAM, SOCOL, ULAQ and WACCM models (3 ensemble members). For each model with more than one ensemble member, their mean value was used. The analysis of TOC presented below was also repeated using the first ensemble member only, as was done in Oman et al. (2010), and it was found that multiple ensembles for the models listed above did not provide any noticeable differences compared to selecting the first ensemble member only.

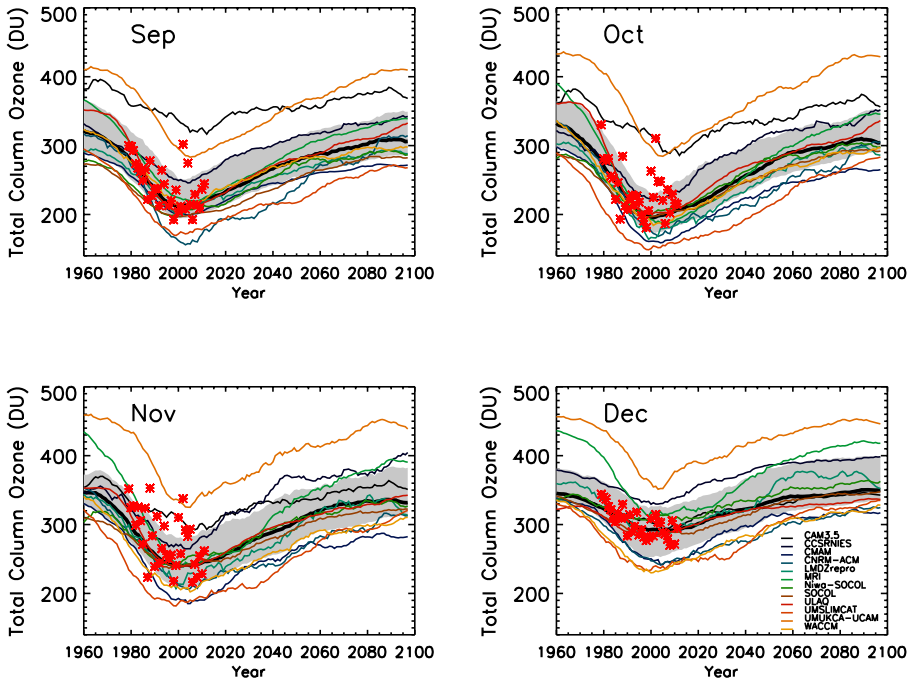

Fig. 1. Total Column Ozone (TOC) time series zonally averaged poleward of 60° S from selected REF-B2 model simulations as indicated on the bottom right panel. Thick black curve is the multi-model median, grey area represents the 95 % confidence limit of the median derived using a bootstrapping method. Data are smoothed with a 15 yr uniformly weighted sliding mean filter. Red stars indicate zonally averaged unsmoothed TOC values poleward of 62.5° S from the TOMS version 8.5 merged ozone dataset (MOD) for 1979–2011.

3 Results

3.1 Trends in total ozone column

CCMVal-2 REF-B2 simulations of TOC from each CCM used in this study are shown in Fig. 1. Model outputs, although widely spread, show a TOC minimum around the year 2000 for all months, which is in agreement with Eyring et al. (2010a). The spread among models is also seen to increase from September to December. The October multi-model median TOC in Fig. 1 is in good qualitative agreement with other CCMVal-2 studies based on the 1965 baseline (Austin et al., 2010b; Eyring et al., 2010a), but quantitatively is ∼50 DU lower then that found in Eyring et al. (2010a). This is possibly due to differences in statistical analysis techniques (TSAM analysis) that was used in that study, and the fact that we have used a subset of the models used in Eyring et al. (2010a) for reasons that have been previously explained. We note that TOC trends for other months shown in Fig. 1 are not directly compared to other studies due to the fact that other studies did not provide such results for September, November and December.

Figure 1 also shows that multi-model median TOC agrees well, within the 95 % confidence interval, with observations in 1979–2011, which are zonally averaged monthly mean TOC values measured by the Total Ozone Mapping Spectrometer (TOMS), Merged Ozone Dataset (MOD) (e.g. Stolarski and Frith, 2006). While some individual model outputs show good agreement with observations, other models produce either too high, or too low TOC values. However, this bias is not consistent for all months considered, except UMUKCA-UCAM that has a consistently high bias for all months, which has been previously reported (SPARC CCMVAL, 2010), and UMSLIMCAT that has a generally low bias for each month, as seen in the initial model trend estimate in Austin et al. (2010b).

As the individual model intercomparison and validation is not part of this work, we did not exclude any model based on their agreement with the TOMS TOC in Fig. 1. Part of the reason for this is that some models are in good agreement with the measured TOC, but not in a good agreement, relative to other models, regarding zonal winds or temperature that are considered later in this study. Nevertheless, we repeated all steps of our analysis presented below for only those 4 models that show a consistent agreement with TOMS TOC for each month considered in this study. These models are LMDZrepro, Niwa-SOCOL, SOCOL, and ULAQ. We found that such narrow selection of models did not significantly change the main results and conclusions of this work, including TOC return dates to the 1965 baseline, and speeds and rates of TOC increase. This could be, in part, due to the fact that the bootstrapping statistical analysis technique employed here minimizes the effect of individual outliers when the multi-model median is calculated. Moreover,

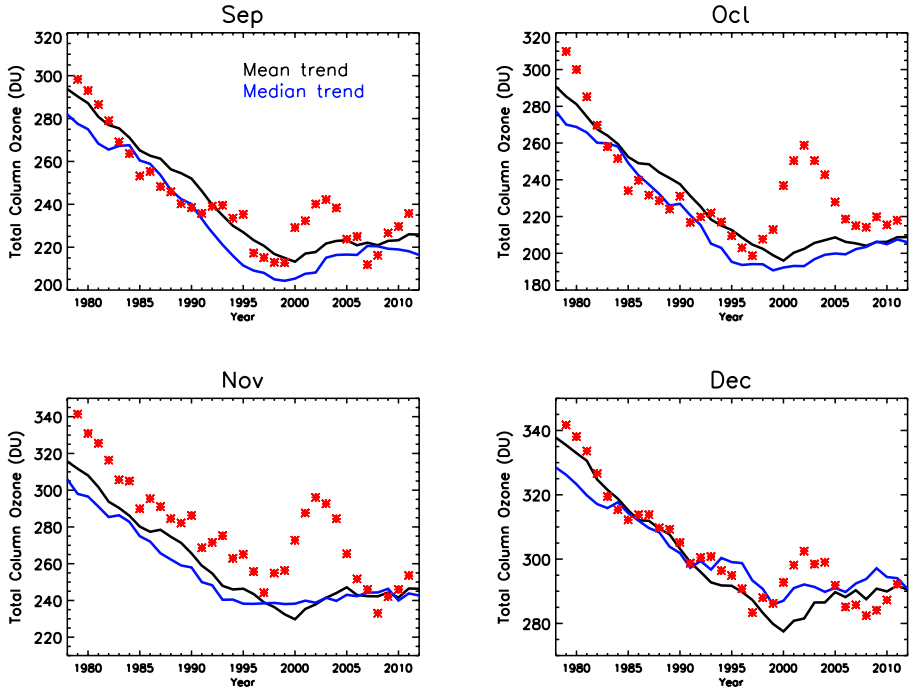

Fig. 2. Multi-model median (blue) and mean (black) TOC time series in comparison with TOMS observations during the 1979–2011 period. Both datasets have been smoothed with a 5 yr uniformly weighted sliding mean filter.

the interannual variability in TOMS data results from variability associated with combined natural and anthropogenic forcings, while CCMVal-2 models consider anthropogenic forcing only. European Centre for Medium-Range Weather Forecasts (ECMWF) ERA-Interim reanalysis data (Dee et al., 2011) in 1979–2010 were also compared with CCMVal-2 TOC values in Fig. 1 (not shown) and, similar to TOMS data, were within the 95 % confidence interval for multi-model median. We also note that CCMVal-2 models used here have a range of grid resolutions (e.g. Morgenstern et al., 2010) that could possibly introduce a statistical bias with different sample populations contributing to individual model TOC trend values that are zonally averaged. In order to investigate this further, time series of ozone mass poleward of 60° S were produced. These results (not shown here) suggest that differences in model grid resolutions do not affect the analysis presented in this work.

Different from CCMVal-2 model data, TOMS data in Fig. 1 are not smoothed. To better illustrate how these datasets compare when treated in the same way, we produced Fig. 2, where both datasets are smoothed with a 5 yr uniformly weighted running filter over the 1979–2011 time period. It appears that multi-model median values do not fully capture the variability seen in the observations, and also that models seem to underestimate TOC values earlier in the observation period for most months, but overestimate the TOC peak depletion values in the beginning of the 21st century. As many previous studies used multi-model mean instead of median, we found it beneficial to show both values and thus demonstrate that there is no apparent advantage of using any of these in the beginning of the simulation period. However, as was mentioned earlier, median values assign lower weight to the most deviating results that occur later in the simulation period.

Multi-model monthly zonal median of TOC deviation from the 1965 baseline for the period of 1960–2100, both a percentage and an absolute deviation, are shown in Figs. 3 and 4, respectively. These results suggest that September–November TOC does not return to its 1965 level by the end of the simulations (2098), but is within ∼1 % (∼3 DU) of the 1965 baseline in 2090. A slight decrease again after 2090 is most likely to be a result of increasing influence of GHG cooling in the lower stratosphere towards the end of the 21st century. December TOC returns to the 1965 baseline in 2079 and continues to increase to approximately 2 % (∼8 DU) above the baseline towards the end of the century. September–November TOC have an earliest return date in the 95 % confidence interval between 2065–2075. The lowest uncertainty range for the December TOC return date is about 30 yr. As all models in this study use the same REF-B2 scenario, the scenario uncertainty is common for all models, and the individual model uncertainties differ. Charlton-Perez et al. (2010) analysed interannual variability, scenario and model uncertainties in four CCMVal-2 models for October and found that for Antarctic latitudes, the combined uncertainty due to the 3 abovementioned factors ranges between

Table 1. Decadal rates and speeds of TOC increase poleward of 60° S as a percentage of 1965 baseline (Case A), in DU/decade (Case B), and as a percentage relative to maximum depletion (baseline minus ∼year 2000 conditions) (Case C). Italicized numbers indicate decades when December TOC has exceeded its 1965 baseline value.

		Decadal TOC rates								
	Decade	2000–2009	2010–2019	2020–2029	2030–3039	2040–2049	2050–2059	2060–2069	2070–2079	2080–2089
Month	Case									
Sep	A	1.99	3.62	4.4	5.29	3.82	2.95	1.64	2.06	2.01
	B	6.45	11.69	14.2	17.07	12.32	9.51	5.3	6.65	6.49
	C	13.11	7.65	15.59	13.54	3.99	6.75	5.97	10.08	0.36
Oct	A	2.42	3.2	5.25	5.48	4.88	4.81	1.52	1.76	2.29
	B	7.97	10.53	17.27	18.01	16.04	15.82	4.98	5.8	7.53
	C	9.43	11.24	5.66	9.55	11.59	2.03	8.91	9.45	16.14
Nov	A	0.97	2.71	4.58	3.72	3.82	4.23	2.51	1.14	0.53
	B	3.42	9.5	16.07	13.04	13.41	14.84	8.82	3.99	1.85
	C	13.27	0.55	8.61	12.74	19.73	13.99	14.52	11.14	14.55
Dec	A	−0.17	2.13	3.52	2.21	2.66	2.29	0.5	*1.06*	*1.16*
	B	−0.57	7.62	12.58	7.9	9.53	8.21	1.78	3.79	*4.14*
	C	22.48	18.04	1.56	3.51	10.73	6.09	6.94	5.12	*6.89*

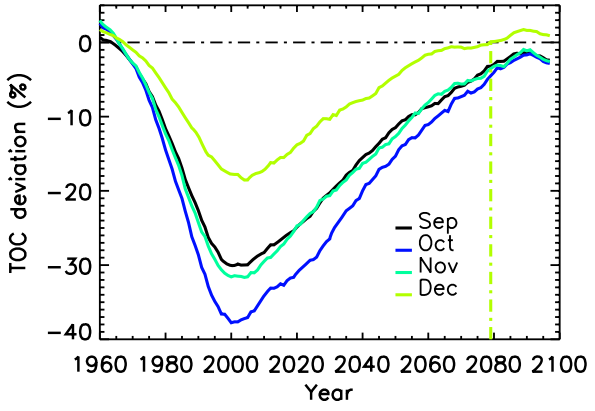

Fig. 3. Time series of multi-model TOC median values for September–December as percent deviations from the 1965 baseline. Curves have been smoothed as described in Fig. 1. TOC return dates to the 1965 baseline are shown by dashed-dotted lines, color-coded by the corresponding month.

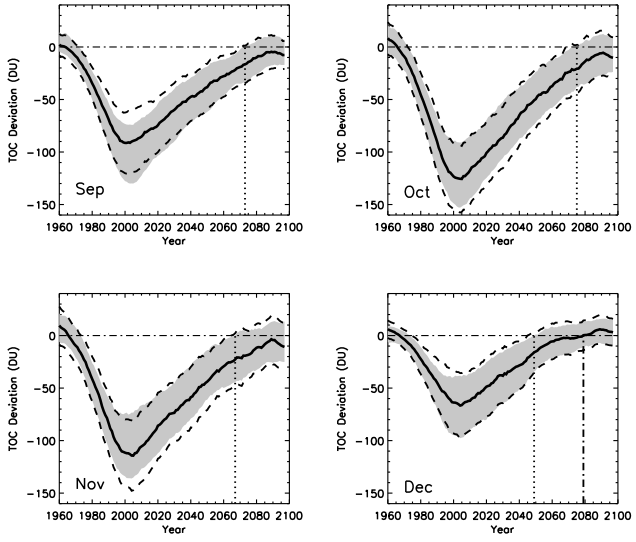

Fig. 4. Time series of deviations for multi-model median TOC from the 1965 baseline for each month. Median TOC return dates are shown by the vertical dot-dashed lines. Shaded area is the 95 % confidence limit of the median with the lower limits return dates shown by vertical dotted lines. Dashed curves show the median absolute deviation range.

15 and 30 DU during the 21st century. Further details are provided on the bottom right panel of their Fig. 3.

According to our results in Fig. 4, the highest ozone depletion of ∼130 DU relative to the 1965 baseline occurs in October. This is about 50 DU larger than the ozone depletion relative to the 1980 baseline in REF-B2 simulations, but comparable to that for the 1960 baseline reported in previous CCMVal-2 model studies (e.g. Austin et al., 2010b; Eyring et al., 2010a). Figure 4 also shows that a minimum TOC value for all months is between 2000 and 2005. Assuming that the ozone hole is defined as a region where TOC values are less than 220 DU (e.g. Newman et al., 2004), we found that its size, calculated from CCMVal-2 model outputs (not shown here), has reached its maximum also between 2000 and 2005.

Figures 3 and 4 suggest that the rate of December TOC increase is slower than that for spring months, even though the recovery of December TOC to baseline occurs earlier. This effect is quantified in Table 1, where the decadal TOC increase speeds (in DU/decade) and rates (in percent relative to baseline and in percent relative to the maximum depletion value) are presented.

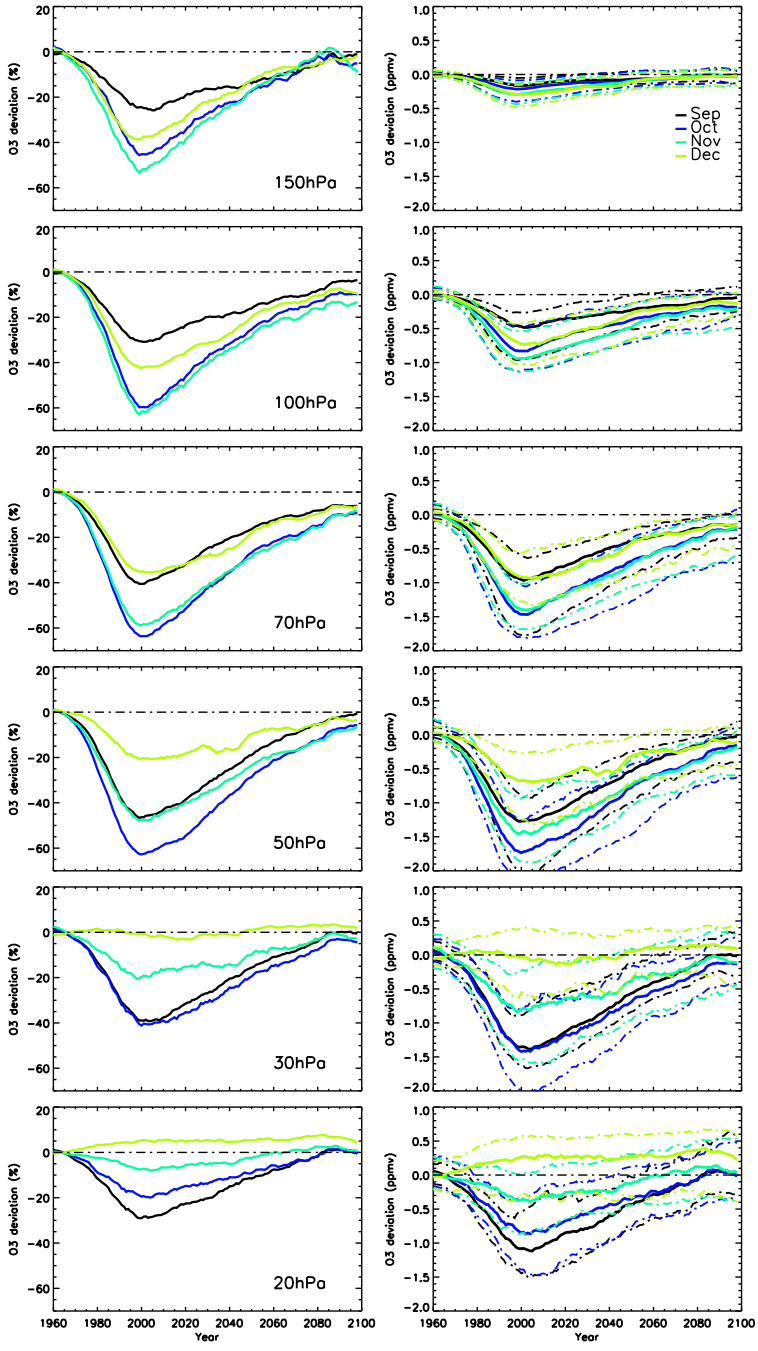

Fig. 5. Deviations of monthly multi-model median ozone VMR from 1965 baseline, zonally averaged poleward of 60° S for all available pressure levels considered by CCMVal-2 models in the range of 20–150 hPa. Left panels – percent deviation from baseline, right panels – absolute deviation from baseline. Dashed lines indicate 95 % confidence level of median. Model data have been smoothed with a 15 yr boxcar filter.

3.2 Trends in Ozone VMR at various stratospheric altitudes

Figure 5 shows vertical profiles for deviations of ozone VMR from baseline in the pressure range where the majority of atmospheric ozone over Antarctica is located and where most of the depletion takes place (e.g. Solomon et al., 2005). In September–October, the SH percentage (absolute) polar ozone loss is greatest at 70 (50) hPa, and in November–December at 100 (70). Thus, the region of the largest ozone loss moves from higher altitudes early in the ozone depletion season to lower altitudes later in the ozone depletion season.

This result is supported by observations of chemical tracers, which show that in spring, air transport within the Antarctic stratosphere is directed downwards (Solomon, 1999). It is also supported by one of the conclusions in SPARC CCMVAL (2010) that by early summer, the breakdown of the polar vortex and the strengthening Brewer–Dobson circulation results in the transport of ozone-rich air to higher latitudes. A recent observational example of this effect – time series of zonally averaged vertical ozone profiles poleward of 60° S in 2002–2009, was reported in Klekociuk et al. (2011) in their Fig. 14a. In that example, the upper edge of the ozone hole descends from ∼19 km in early October to ∼15 km in early December.

Based on 25 yr of ozonesonde measurements at the South Pole and the Georg-Forster/Neumayer Antarctic stations, Hassler et al. (2011) investigated minimum daily ozone VMR at 50 hPa from late September until early October. Their data, as a vertical profile of percent ozone loss for 5 yr averages between day 235 and 270 (see their Fig. 5c) indicate that the loss rates increased at 150–50 hPa, but decreased at 40–20 hPa. CCMVal-2 model projections for the same months show the maximum ozone loss occurring between 70 and 50 hPa, which agrees well with measurements of Hassler et al. (2011).

At 150 hPa, the deviation of ozone VMR from baseline is smallest, and a return to near baseline values occurs in ∼2065 for all months. Above 150 hPa, as the pressure decreases (altitude increases), the December, and to a lesser extent November, ozone shows less depletion. December ozone VMR at 70 hPa, in comparison with the spring months, begins to show a noticeable slow down in the rate (speed) of its increase. This effect becomes even more pronounced at 50 hPa. At 30 hPa, the December ozone is not significantly depleted – its VMR deviates from the baseline by 0.2 ppmv, or less, which is about 5 % of the baseline value. At 20 hPa, the December ozone VMR remains above the baseline, and the November ozone VMR is lower than the baseline by less than 0.4 ppmv (also about 5 % of the baseline value). These are the likely reasons for the observed, somewhat slower December TOC increase in 2010–2050 shown in Figs. 3 and 4 and in Table 1.

3.3 Trends in stratospheric temperatures and winds

In order to better understand projected Antarctic ozone recovery trends, particularly the slower TOC increase in December, we investigate trends in stratospheric temperature and winds (Figs. 6 and 7, respectively). These parameters, also provided by CCMVal-2 model simulations, relate to changes in the size and strength of the polar vortex as halogen concentrations decrease and GHG concentrations increase (e.g. Waugh and Polvani, 2010). Monthly zonal mean fields for these metrics were obtained at the same pressure levels as ozone VMR in Fig. 5. Zonal mean temperatures were calculated poleward of 60° S, whereas zonal mean zonal wind speeds were averaged over the 50°–70° S range. This range covers latitudes where the edge of the polar vortex is expected to be throughout the 21st century.

Figure 6 suggests a general decrease in the lower stratospheric temperatures until 2000, when ozone was decreasing as well. Figures 5 and 6 indicate a correlation between lower temperatures and lower ozone levels. Such a correlation is likely to arise from temperature-dependent heterogeneous polar stratospheric chemistry, including the production of gaseous Cl_2 on polar stratospheric clouds (PSCs) prior to photolysis, together with horizontal and vertical transport of air caused by planetary waves (e.g. Wirth, 1993; Solomon et al., 2005). At 150 hPa, CCMVal-2 multi-model temperatures return to a 1965 baseline by the end of the 21st century for September–October months. For all other altitudes and months examined in this study, stratospheric temperatures remain below the baseline value until the end of the 21st century, which can be attributed to the projected increase in GHG concentrations as stated in the A1B scenario (IPCC, 2000). CCMVal-2 models in the REF-B2 simulations suggest that during the ozone decrease period of 1970–2000, temperature median trends at 100 hPa were approximately $-0.5\,\mathrm{K\,decade^{-1}}$ for September–October and $-1.5\,\mathrm{K\,decade^{-1}}$ for November, giving a spring average of around $-0.8\,\mathrm{K\,decade^{-1}}$. During December, the temperature trend was about $-1\,\mathrm{K\,decade^{-1}}$.

Randel et al. (2009) analyzed satellite, radiosonde and lidar temperature observations in 1979–2007 at 100 hPa over the same latitude range and found a similar cooling trend of about $-1\,\mathrm{K\,decade^{-1}}$ for spring months and $-1.5\,\mathrm{K\,decade^{-1}}$ for summer months. The period of maximum temperature deviation from baseline in Fig. 6 generally coincides with the period of maximum depletion in ozone VMR observed in Fig. 5. December temperatures have the largest deviation from baseline at 100 hPa, November at 70 hPa, October at 50 hPa, and September at 20 hPa. These deviations in temperature correlate with deviations in ozone at the same pressure levels for most months. September temperature is at its minimum at the end of the 21st century rather than during the peak ozone depletion around the year ∼2000. December temperature also shows a slower increase at 50–70 hPa, in agreement with the slower December TOC recovery.

At 30 hPa, December temperatures show no significant trend during the period of ozone decrease until about 2000. At altitudes above 30 hPa, an initial increase in December temperature is followed by cooling towards the end of the 21st century. For this period, December ozone VMR in Fig. 5 shows a small decrease and then an increase at higher pressure levels. Both December ozone and December temperature time series indicate a reversal in the radiative effect of ozone. In the lowermost stratosphere, ozone and temperature correlate: a decrease in ozone levels leads to a decrease in temperature. But at higher altitudes they anti-correlate: an increase in ozone is associated with a radiative cooling

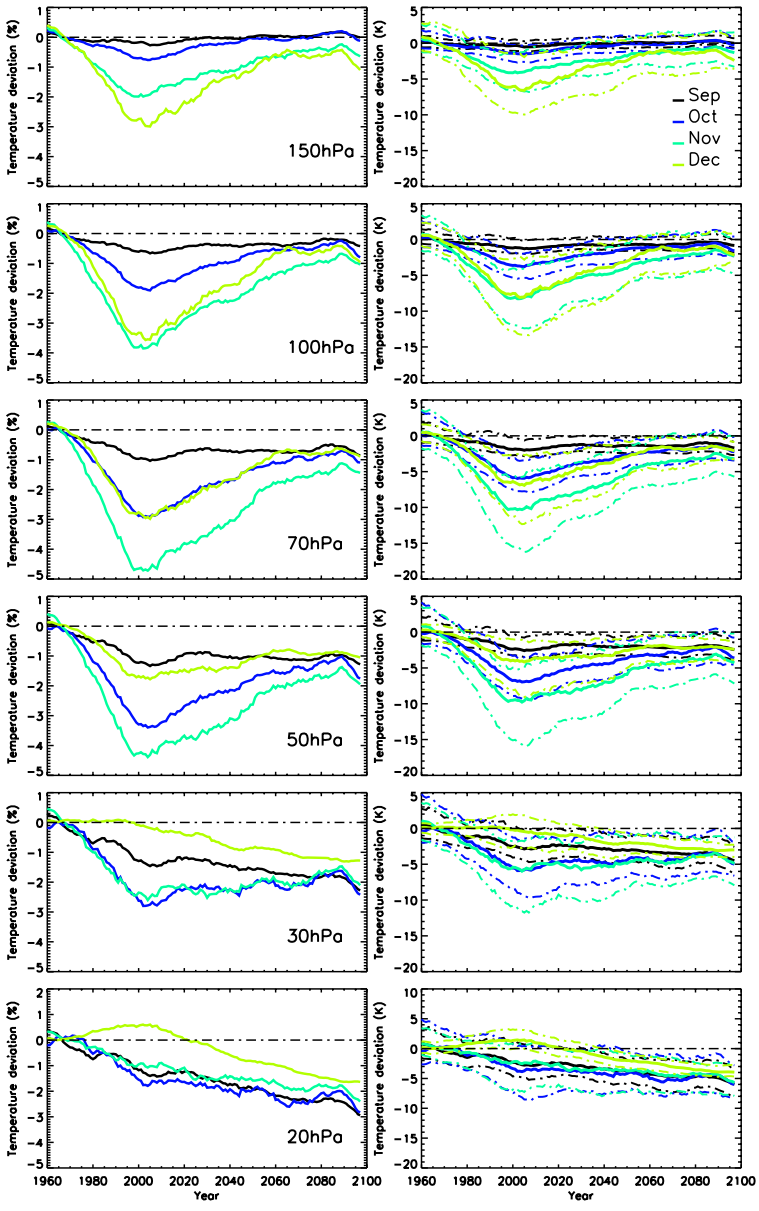

Fig. 6. Same as in Fig. 5, but for multi-model median temperatures.

observed from ∼2000 for all months. This anti-correlation is seen at 20 hPa for all months and also down to 30 hPa for December. As will be discussed later, such a decrease in temperature could be related to CO_2-induced cooling, which in turn leads to a slowdown in ozone destruction reactions (e.g. Shepherd and Jonsson, 2008).

During the period of 2000–2080, lower stratospheric temperatures in December are influenced by increasing ozone with warming occurring at altitudes up to 50 hPa. However, temperatures at this altitude range also begin to plateau somewhat earlier than ozone VMR, around 2065 for 150–70 hPa. At altitudes corresponding to 50 hPa, December temperature increase is slow from 2000 onwards. Above these heights, stratospheric cooling increases with increasing altitude, with no temperature recovery to baseline due to effects of long-term CO_2 cooling. If lower stratospheric cooling associated with ozone depletion could lead to a strengthening of the polar vortex, then warming associated with ozone recovery would decrease the stability of the vortex and affect future persistence of the vortex into early summer. To analyze this effect, monthly zonal mean zonal winds were considered at the same pressure levels as temperatures and ozone VMR in Fig. 7. Waugh et al. (1999) found that similar to potential vorticity (PV), zonal wind is a useful diagnostics in assessing the breakup of the polar vortex, although not as highly derivative. As noted earlier, we consider wind data averaged across

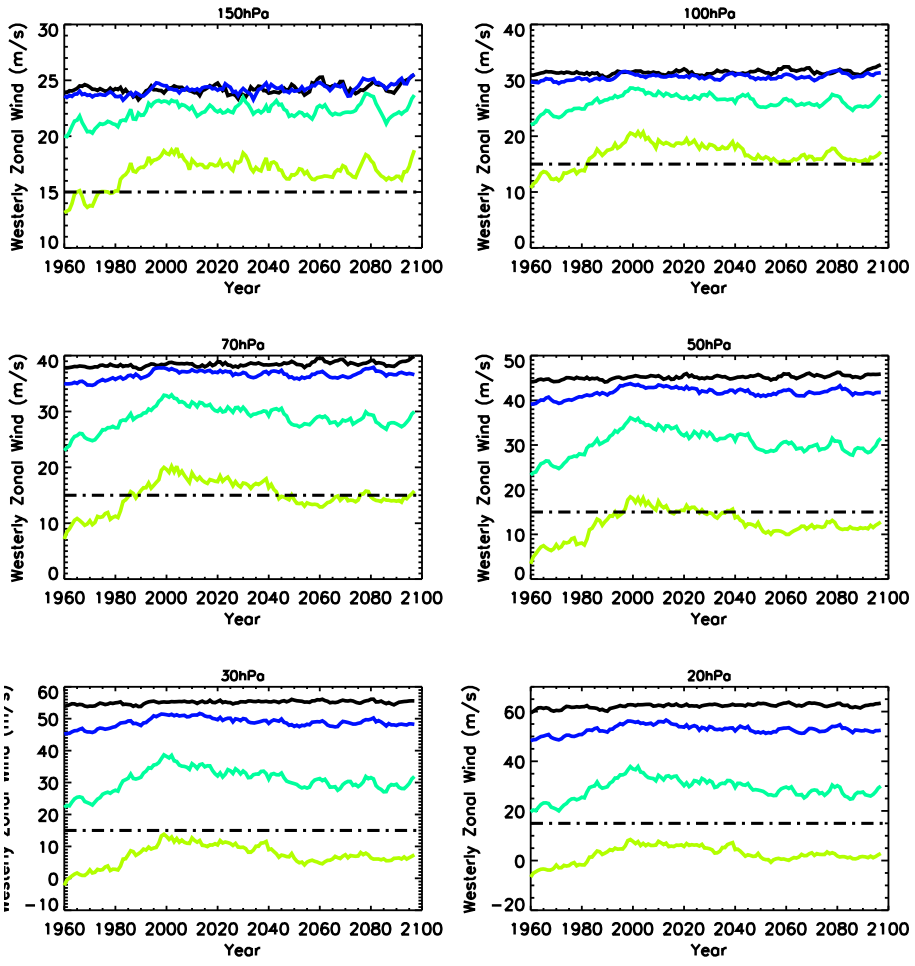

Fig. 7. Time series of monthly zonal mean zonal wind speed averaged across 50°–70° S at 20-150 hPa. Dot-dashed lines indicate the minimum wind velocity of 15 m s^{-1} that identifies the polar vortex edge. Colors correspond to same months as in Fig. 5.

50°–70° S, which encompasses the location of the edge of the polar vortex (e.g. Lee et al., 2001). Wind speeds across smaller 5° latitude bins were also analyzed in this work (not shown), and the resulting trends were similar to those averaged over the 50°–70° S region.

A minimum wind speed of 15 ms^{-1}, below which the vortex is considered to have broken up, is used in this study, similar to the method used in Nash et al. (1996). For all pressure levels analysed, spring months winds indicate that the polar vortex is present over the entire time period. For December, model outputs suggest that at heights above 50 hPa, the polar vortex is broken up. However, at altitudes below 50 hPa, the December wind speed of $\geq$ 15 ms^{-1} indicates that the vortex edge is present until the middle of the 21st century. As the polar vortex collapses in early summer, its edge could either disappear, or first shift poleward, and then disappear. To analyze whether the December zonal mean wind speed exceeded the 15 ms^{-1} limit at higher latitudes compared to what is shown in Fig. 7, monthly zonal wind data were also considered at higher latitudes of 70°–80° S. These results (not shown) revealed trends in zonal wind speeds at each pressure level very similar to those in Fig. 7, suggesting that stratospheric polar vortex quickly collapses in December.

Figure 7 indicates that increasing polar westerlies, associated with ozone depletion, are seen in the lower stratosphere during November and December until ∼2000. During the ozone recovery period, there is a corresponding decrease in polar westerlies. When compared with results for TOC and ozone VMR in Figs. 3, 4 and 5, there is about a one month time lag in zonal wind response to changes in ozone VMR. Overall, there is no significant trend in zonal winds for the months of September–October. Monier and Weare (2011) found similar results with the ECMWF ERA-40 reanalysis data over the time period of 1980–2001, with a strengthening westerly wind associated with ozone depletion via the thermal wind balance.

Zonal winds were also considered with respect to trends seen in the monthly TOC values. The 1965 baseline wind value u_{base} and a mean peak value u_{peak} between 2000–2005 are used to produce the time series for normalized zonal wind

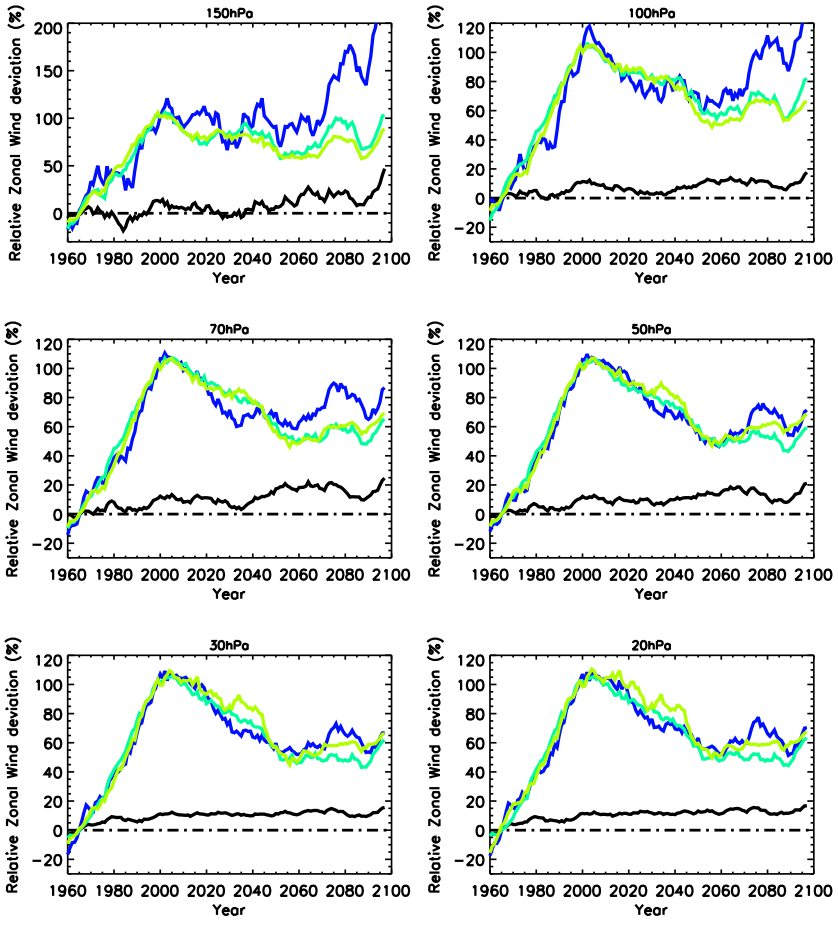

Fig. 8. Normalized time series of percent deviation of zonal mean zonal wind speed averaged over 50°–70° S. For full description see text. The September wind data have been scaled, divided by 10 at all altitudes. Colors correspond to same months as in Fig. 5.

percentage deviation, δ, as shown in Fig. 8. This normalized wind percentage deviation of annual wind speed values u(t) is calculated as

$$\delta = \left(\frac{u(t) - \overline{u}_{\text{base}}}{u_{\text{peak}} - \overline{u}_{\text{base}}} \right) \times 100\,\%. \quad (1)$$

As September wind data had high absolute wind values but small variability, in order to be shown together with other months, they were scaled by a factor of 10 at all altitudes.

Figure 8 suggests that the percent increase in zonal wind speed during the ozone depletion period is very similar between all months. By 2100, model projections indicate a net increase in wind speeds for all months, compared to the 1965 baseline values, due to an indirect effect of increasing surface GHG concentrations via temperature changes. The increasing effect of GHG is also seen in the secondary peak in zonal median wind at all pressure levels for all months except September.

There is evidence that austral summer wind speeds increase significantly, both in the troposphere and in the stratosphere, due to decreasing ozone and increasing GHG concentrations (Thompson and Solomon, 2002; Shindall and Schmidt, 2004; Perlwitz et al., 2008; Son et al., 2010). According to these studies, future changes in SH atmospheric circulation due to ozone recovery are expected to be opposed by increases in tropospheric GHG. However, effects from increasing ozone concentrations and decreasing ozone hole size will still dominate at Antarctic latitudes until 2100.

4 Discussion and conclusions

The presented analysis of CCM Val-2 model simulations indicates that due to combined effects of increasing GHG and decreasing halogen levels in the 21st century, Antarctic TOC will not return to its 1965 baseline in September–November, but will return to baseline in December in ∼2079. The recovery of December TOC to baseline has an uncertainty of ∼30 yr within a 95 % confidence level. We note that the 1965 baseline is a somewhat arbitrary value, and thus the fact that September–November ozone will not return to its 1965 level by 2100 does not indicate that the ozone depletion due to ODSs will still be significant. As seen in Figs. 3 and 4, by

2100, Antarctic ozone is still appreciably affected by ODSs (as dictated by the adjusted WMO A1 scenario), and the impact of increasing GHGs on ozone depletion is about as large as that of ODSs, but opposite in sign.

TOC increase rates and speeds in Table 1 (Cases A and B) are low for all months in 2000–2009, and those for December are often significantly lower, up to factor of 10, compared to other months. Model simulations suggest that in early spring, the maximum contribution to decrease in TOC comes from ozone depletion at higher altitudes, and in early summer – from ozone depletion at lower altitudes. This is in agreement with various independent observations discussed in Sect. 3.2. At 50–100 hPa, December ozone does not return to the 1965 baseline by 2100, in contrast to the return date for December TOC (∼2079). Furthermore, slower rates of December TOC increase projected for certain decades, as shown in Table 1, originate from slower rates of December ozone VMR increase at 50–100 hPa This slower increase is especially evident at 50–70 hPa (these are also the altitudes of highest December ozone depletion). At 20–30 hPa, December ozone VMR show little variations during the 21st century.

Multi-model median trends in monthly temperatures correlate well with ozone within the lowermost stratosphere (70–150 hPa), particularly during October–November – as expected for temperature-dependent polar stratospheric chemistry where temperatures rise with the ozone increase. However, at altitudes corresponding to 20–30 hPa, there is a reversed radiative effect due to a combined effect of increased GHG and decreased ODS concentrations. At 50–100 hPa, model simulations indicate that December temperatures stop increasing in ∼2060 and remain nearly constant until the end of the century. During this time period, December ozone VMR is still slowly increasing, indicating no apparent dependence on temperature and a weakening of the polar vortex as ozone-rich air from lower latitudes is moving to these pressure levels.

A decrease in temperature in the lower polar stratosphere, particularly within the polar vortex, results in an increase in the meridional temperature gradient at the vortex edge and thus enhances westerly zonal winds in this region. Circumpolar westerly zonal winds show an increase in magnitude during the period of ozone depletion with a corresponding decrease during ozone recovery for all months considered. Using a $15\,\mathrm{ms}^{-1}$ minimum in zonal wind speed as a proxy for the polar vortex edge, the polar vortex was found to be present for all spring months across all altitudes considered, but broken up by December above 50 hPa. In the lowermost stratosphere, model simulations for December indicate a persisting vortex well into early summer, especially during the peak ozone depletion period around the year 2000. At pressures ≥ 100 hPa, zonal winds suggest a presence of the vortex in December until the end of the model simulations. At 50-70 hPa, the December vortex lasts until ∼2045, and after that date the cooling rate start to decrease, as shown in Fig. 6.

A delay in the vortex breakup, indicated by CCMVal-2 multi-model median wind time series, leads to a delay in TOC increase during December. Anthropogenic ODS emissions dominate in the lowermost stratosphere, while CO_2 cooling dominates at higher altitudes. However, an increase in GHG concentrations may start affecting ozone levels in the lowermost stratosphere towards the end of the 21st century, when ODS no longer have a significant influence on atmospheric ozone over Antarctica. We also note that our analysis of ozone recovery is based on zonal averages, and thus the previously reported zonal asymmetries in the TOC field (e.g. Grytsai et al., 2007) may lead to some local variations in ozone return dates.

At altitudes above ∼10 hPa, stratospheric cooling can lead to a decreased efficiency of chemical ozone destruction, and therefore to an increased ozone VMR (e.g. Finger et al., 1995). At altitudes below 10 hPa, increased cooling promotes more heterogeneous reactions. However, their efficiency also depends on water vapour concentrations as discussed by Shindell (2001). Model results analyzed here show that such anti-correlation can be seen down to altitudes corresponding to 30 hPa. Shepherd and Jonsson (2008) suggested that global mean temperature variations should be considered in terms of changes in CO_2 and ODS, rather than ozone. They found that during 2010–2040, a period of rapid ODS decrease, up to 40 % of the increase in mean global upper stratospheric ozone (between 50 and 0.5 hPa) is attributed to CO_2 cooling. But during the depletion period of 1975–1995, only ∼10 % of ozone loss is attributed to CO_2 cooling, which is much smaller compared with the effect of ODS increases alone. However, these global effects of increasing CO_2 on ozone levels may not be the same on a regional scale. For example, it was found that lower stratospheric ozone averaged over the Southern Hemisphere mid-latitudes decreases with increasing GHG concentrations (Waugh et al. 2009). Multi-model trends obtained in this study indicate that during spring months, decreasing ODSs lead to increasing ozone. But as the end of the 21st century is approaching, December ozone is less influenced by halogens and more influenced by increasing GHG, which is evidenced by a decreased radiative heating that occurs in the lower stratosphere.

CCMVal-2 models indicate a response of zonal winds to recovering ozone, namely a decrease in wind speed with increasing ozone VMR. A wind response to changes in temperature, associated with ozone concentration, has about a one-month time lag: maximal ozone gradients are seen in October–November and maximum wind gradients are seen a month later, in November–December. This pattern is also reported by Akiyoshi et al. (2009), based on observations and a CCM simulation (CCSRNIES). Persistence of the polar vortex into the summer months could also be linked to decreasing planetary wave activity, which was described in Monier and Weare (2011). The breakdown of the polar westerlies is induced by dynamical heating from breaking planetary waves, and the timing of this breakdown in early summer

can influence the propagation of gravity waves into the mesosphere, thus potentially affecting the strength of the mesospheric branch of the Brewer–Dobson circulation (Smith et al., 2010). In this study, December westerly zonal winds over a 100 yr period (between ∼1990 and ∼2090) show a long-term decrease with an earlier vortex breakup at the end of the model simulations compared to the peak ozone depletion period, particularly between 50 and 70 hPa. This is similar to the result of Deushi and Shibata (2011). Using the MRI model, they found a maximum decrease in mean age of air at 50 hPa in December due to lower stratospheric wave forcing.

Acknowledgements. We acknowledge the modeling groups for making their simulations available for this analysis, the Chemistry-Climate Model Validation Activity (CCMVal) for the World Climate Research Programme's (WCRP) Stratospheric Processes and their Role in Climate (SPARC) project for organizing and coordinating the model data analysis activity, and the British Atmospheric Data Centre (BADC) for collecting and archiving the CCMVal model output. TOMS data are freely available from the NASA website http://acd-ext.gsfc.nasa.gov/Data_services/merged/. This work was sponsored in part by the Australian Antarctic Division Division under Australian Antarctic Science projects 737 and 2699. Part of this work was also supported by the Commonwealth Department of Environment, Water, Heritage and the Arts, grant 2008/02103.

Edited by:

References

Akiyoshi, H., Zhou, L. B., Yamashita, Y., Sakamoto, K., Yoshiki, M., Nagashima, T., Takahashi, M., Kurokawa, J., Takigawa, M., and Imamura, T.: A CCM simulation of the breakup of the Antarctic polar vortex in the years 1980–2004 under the CCMVal scenarios, J. Geophys. Res., 114, D03103, doi:10.1029/2007JD009261, 2009.

Austin, J., Scinocca, J., Plummer, D., Oman, L., Waugh, D., Akiyoshi, H., Bekki, S., Braesicke, P., Butchart, N., Chipperfield, M., Cugnet, D., Dameris, M., Dhomse, S., Eyring, V., Frith, S., Garcia, R. R., Garny, H., Gettelman, A., Hardiman, S. C., Kinnison, D., Lamarque, J. F., Mancini, E., Marchand, M., Michou, M., Morgenstern, O., Nakamura, T., Pawson, S., Pitari, G., Pyle, J., Rozanov, E., Shepherd, T. G., Shibata, K., Teyssedre, H., Wilson, R. J., and Yamashita, Y.: Decline and recovery of total column ozone using a multimodel time series analysis, J. Geophys. Res., 115, D00M10, doi:10.1029/2010JD013857, 2010a.

Austin, J., Struthers, H., Scinocca, J., Plummer, D. A., Akiyoshi, H., Baumgaertner, A. J. G., Bekki, S., Bodeker, G. E., Braesicke, P., Br"uhl, C., Butchart, N., Chipperfield, M. P., Cugnet, D., Dameris, M., Dhomse, S., Frith, S., Garny, H., Gettelman, A., Hardiman, S. C., Jöckel, P., Kinnison, D., Kubin, A., Lamarque, J. F., Langematz, U., Mancini, E., Marchand, M., Michou, M., Morgenstern, O., Nakamura, T., Nielsen, J. E., Pitari, G., Pyle, J., Rozanov, E., Shepherd, T. G., Shibata, K., Smale, D., Teyssèdre, H., and Yamashita, Y.: Chemistry-climate model simulations of spring Antarctic ozone, J. Geophys. Res., 115, D00M11, doi:10.1029/2009JD013557, 2010b.

Buchart, N., Charlton-Perez, A. J., Cionni, I., Hardiman, S. C., Haynes, P. H., Krüger, K., Kushner, P. J., Newman, P. A., Osprey, S. M., Perlwitz, J., Sigmond, M., Wang, L., Akiyoshi, H., Austin, J., Bekki, S., Baumgaertner, A., Braesicke, P., Brühl, C., Chipperfield, M., Dameris, M., Dhomse, S., Eyring, V., Garcia, R., Garny, H., JöCkel, P., Lamarque, J. F., Marchand, M., Michou, M., Morgenstern, O., Nakamura, T., Pawson, S., Plummer, D., Pyle, J., Rozanov, E., Scinocca, J., Shepherd, T. G., Shibata, K., Smale, D., Teyss'edre, H., Tian, W., Waugh, D., and Yamashita, Y.: Multimodel climate and variability of the stratosphere, J. Geophys. Res., 116, D05102, doi:10.1029/2010JD014995, 2011.

Charlton-Perez, A. J., Hawkins, E., Eyring, V., Cionni, I., Bodeker, G. E., Kinnison, D. E., Akiyoshi, H., Frith, S. M., Garcia, R., Gettelman, A., Lamarque, J. F., Nakamura, T., Pawson, S., Yamashita, Y., Bekki, S., Braesicke, P., Chipperfield, M. P., Dhomse, S., Marchand, M., Mancini, E., Morgenstern, O., Pitari, G., Plummer, D., Pyle, J. A., Rozanov, E., Scinocca, J., Shibata, K., Shepherd, T. G., Tian, W., and Waugh, D. W.: The potential to narrow uncertainty in projections of stratospheric ozone over the 21st century, Atmos. Chem. Phys., 10, 9473–9486, doi:10.5194/acp-10-9473-2010, 2010.

Dee, D. P., Uppala, S. M., Simmons, A. J., Berrisford, P., Poli, P., Kobayashi, S., Andrae, U., Balmaseda, M. A., Balsamo, G., Bauer, P., Bechtold, P., Beljaars, A. C. M., van de Berg, L., Bidlot, J., Bormann, N., Delsol, C., Dragani, R., Fuentes, M., Geer, A. J., Haimberger, L., Healy, S. B., Hersbach, H., Hólm, E. V., Isaksen, L., Kaallberg, P., Köhler, M., Matricardi, M., McNally, A. P., Monge-Sanz, B. M., Morcrette, J. J., Park, B.-K., Peubey, C., de Rosnay, P., Tavolato, C., Thépaut, J. N., and Vitart, F.: The ERA-Interim reanalysis: configuration and performance of the data assimilation system, Q. J. Roy. Meteor. Soc., 137, 553–597, doi:10.1002/qj.828, 2011.

Deushi, M. and Shibata, K.: Impacts of increases in greenhouse gases and ozone recovery on lower stratospheric circulation and the age of air: Chemistry-climate model simulations up to 2100, J. Geophys. Res., 116, D07107, doi:10.1029/2010JD015024, 2011.

Eyring, V., Cionni, I., Bodeker, G. E., Charlton-Perez, A. J., Kinnison, D. E., Scinocca, J. F., Waugh, D. W., Akiyoshi, H., Bekki, S., Chipperfield, M. P., Dameris, M., Dhomse, S., Frith, S. M., Garny, H., Gettelman, A., Kubin, A., Langematz, U., Mancini, E., Marchand, M., Nakamura, T., Oman, L. D., Pawson, S., Pitari, G., Plummer, D. A., Rozanov, E., Shepherd, T. G., Shibata, K., Tian, W., Braesicke, P., Hardiman, S. C., Lamarque, J. F., Morgenstern, O., Pyle, J. A., Smale, D., and Yamashita, Y.: Multimodel projections of stratospheric ozone in the 21st century, J. Geophys. Res., 112, D16303, doi:10.1029/2006JD008332, 2007.

Eyring, V., Cionni, I., Bodeker, G. E., Charlton-Perez, A. J., Kinnison, D. E., Scinocca, J. F., Waugh, D. W., Akiyoshi, H., Bekki, S., Chipperfield, M. P., Dameris, M., Dhomse, S., Frith, S. M., Garny, H., Gettelman, A., Kubin, A., Langematz, U., Mancini, E., Marchand, M., Nakamura, T., Oman, L. D., Pawson, S., Pitari, G., Plummer, D. A., Rozanov, E., Shepherd, T. G., Shibata, K., Tian, W., Braesicke, P., Hardiman, S. C., Lamarque, J. F., Morgenstern, O., Pyle, J. A., Smale, D., and Yamashita, Y.: Multimodel assessment of stratospheric ozone return dates and ozone recovery in CCMVal-2 models, Atmos. Chem. Phys., 10, 9451-

9472, doi:10.5194/acp-10-9451-2010, 2010a.

Eyring, V., Cionni, I., Lamarque, J. F., Akiyoshi, H., Bodeker, G. E., Charlton-Perez, A. J., Frith, S. M., Gettelman, A., Kinnison, D. E., Nakamura, T., Oman, L. D., Pawson, S., and Yamashita, Y.: Sensitivity of 21st century stratospheric ozone to greenhouse gas scenarios, Geophys. Res. Lett., 37, L16801, doi:10.1029/2010GL044443, 2010b.

Farman, J. C., Gardner, B. G., and Shanklin, J. D.: Large losses of total ozone in Antarctica reveal seasonal ClO_X/NO_X interaction, Nature, 315, 207–210, 1985.

Finger, F. G., Nagatani, R. M., Gelman, M. E., Long, C. S., and Miller, A. J.: Consistency between variations of ozone and temperature in the stratosphere, Geophys. Res. Lett., 22, 3477–3480, 1995.

Grytsai, A. V., Evtushevsky, O. M., Agapitov, O. V., Klekociuk, A. R., and Milinevsky, G. P.: Structure and long-term change in the zonal asymmetry in Antarctic total ozone during spring, Ann. Geophys., 25, 361–374, doi:10.5194/angeo-25-361-2007, 2007.

Hassler, B., Daniel, J. S., Johnson, B. J., Solomon, S., and Oltmans, S. J.: An assessment of changing ozone loss rates at South Pole: Twenty-five years of ozonesonde measurements, J. Geophys. Res., 116, D22301, doi:10.1029/2011JD016353, 2011.

Hofmann, D. J., Oltmans, S. J., Harris, J. M., Johnson, B. J., and Lathrop, J. A.: Ten years of ozonesonde measurements at the south pole: implications for recovery of springtime Antarctic ozone, J. Geophys. Res., 102, 8931–8944, 1997.

IPCC (Intergovernmental Panel on Climate Change): Special report on emissions scenarios: a special report of Working Group III of the Intergovernmental Panel on Climate Change, 599 pp., Cambridge University Press, Cambridge, UK, 2000.

Jones, A. E. and Shanklin, J. D.: Continued decline of total ozone over Halley, Antarctica, since 1985, Nature, 376, 409–411, 1995.

Klekociuk, A. R., Tully, M. B., Alexander, S. P., Dargaville, R. J., Deschamps, L. L., Fraser, P. J., Gies, H. P., Henderson, S. I., Javorniczky, J., Krummel, P. B., Petelina, S. V., Shanklin, J. D., Siddaway, J. M., and Stone, K. A.: The Antarctic ozone hole during 2010, Aust. Meteor. Ocean. J., 61, 253–267, 2011.

Lee, A. M., Roscoe, H. K., Jones, A. E., Haynes, P. H., Shuckburgh, E. F., Morrey, M. W., and Pumphrey, H. C.: The impact of the mixing properties within the Antarctic stratospheric vortex on ozone loss in spring, J. Geophys. Res., 106, 3203–3211, 2001.

Monier, E. and Weare, B. C.: Climatology and trends in the forcing of the stratospheric zonal-mean flow, Atmos. Chem. Phys., 11, 12751–12771, doi:10.5194/acp-11-12751-2011, 2011.

Morgenstern, O., Giorgetta, M. A., Shibata, K., Eyring, V., Waugh, D. W., Shepherd, T. G., Akiyoshi, H., Austin, J., Baumgaertner, A. J. G., Bekki, S., Braesicke, P., Brühl, C., Chipperfield, M. P., Cugnet, D., Dameris, M., Dhomse, S., Frith, S. M., Garny, H., Gettelman, A., Hardiman, S. C., Hegglin, M. I., Jöckel, P., Kinnison, D. E., Lamarque, J. F., Mancini, E., Manzini, E., Marchand, M., Michou, M., Nakamura, T., Nielsen, J. E., Olivié, D., Pitari, G., Plummer, D. A., Rozanov, E., Scinocca, J. F., Smale, D., Teyssèdre, H., Toohey, M., Tian, W., and Yamashita, Y.: Review of the formulation of present-generation stratospheric chemistry-climate models and associated external forcings, J. Geophys. Res., 115, D00M02, doi:10.1029/2009JD013728, 2010.

Nash, E. R., Newman, P. A., Rosenfield, J. E., and Schoeber, M. R.: An objective determination of the polar vortex usig Ertel's potential vorticity, J. Geophys. Res., 101, 9471–9478, 1996.

Newman, P. A. and Kawa, S. R.: On the size of the Antarctic ozone hole, Geophys. Res. Lett., 31, L21104, doi:10.1029/2004GL020596, 2004.

Newman, P. A., Nash, E. R., Kawa, S. R., Montzka, S. A., and Schauffler, S. M.: When will the Antarctic ozone hole recover?, Geophys. Res. Lett., 33, L12814, doi:10.1029/2005GL025232, 2006.

Newman, P. A., Daniel, J. S., Waugh, D. W., and Nash, E. R.: A new formulation of equivalent effective stratospheric chlorine (EESC), Atmos. Chem. Phys., 7, 4537–4552, doi:10.5194/acp-7-4537-2007, 2007.

Oman, L. D., Plummer, D. A., Waugh, D. W., Austin, J., Scinocca, J. F., Douglass, A. R., Salawitch, R. J., Canty, T., Akiyoshi, H., Bekki, S., Braesicke, P., Butchart, N., Chipperfield, M. P., Cugnet, D., Dhomse, S., Eyring, V., Frith, S., Hardiman, S. C., Kinnison, D. E., Lamarque, J. F., Mancini, E., Marchand, M., Michou, M., Morgenstern, O., Nakamura, T., Nielsen, J. E., Olivié, D., Pitari, G., Pyle, J., Rozanov, E., Shepherd, T. G., Shibata, K., Stolarski, R. S., Teyssèdre, H., Tian, W., Yamashita, Y., and Ziemke, J. R.: Multimodel assessment of the factors driving stratospheric ozone evolution over the 21st century, J. Geophys. Res., 115, D24306, doi:10.1029/2010JD014362, 2010.

Perlwitz, J., Pawson, S., Fogt, R. L., Nielsen, E., and Neff, W. D.: Impact of stratospheric ozone recovery on Antarctic climate, Geophys. Res. Lett., 35, L08714, doi:10.1029/2008GL033317, 2008.

Randel, W. J. et al.: An update of observed stratospheric trends, J. Geophys. Res., 114, D02107, doi:10.1029/2008JD010421, 2009.

Scinocca, J. F., Stephenson, D. B., Bailey, T. C., and Austin, J.: Estimates of past and future ozone trends from multi-model simulations using a flexible smoothing spline methodology, J. Geophys. Res., 115, D00M12, doi:10.1029/2009JD013622, 2010.

Shepherd, T. G. and Jonsson, A. I.: On the attribution of stratospheric ozone and temperature changes to changes in ozone-depleting substances and well-mixed greenhouse gases, Atmos. Chem. Phys., 8, 1435–1444, doi:10.5194/acp-8-1435-2008, 2008.

Shindell, D. T.: Climate and ozone response to increased stratospheric water vapor, Geophys. Res. Lett., 28, 1551–1554, doi:10.1029/1999GL011197, 2001.

Shindell, D. T. and Schimdt, G. A.: Southern Hemisphere climate response to ozone changes and greenhouse gas increases, Geophys. Res. Lett., 31, L18209, doi:10.1029/2004GL020724, 2004.

Smith, A. K., Garcia, R. R., Marsh, D. R., Kinnison, D. E., and Richter, J. H.: Simulations of the response of mesospheric circulation and temperature to the Antarctic ozone hole, Geophys. Res. Lett., 37, L22803, doi:10.1029/2010GL045255, 2010.

Solomon, S.: Stratospheric ozone depletion: a review of concepts and history, Rev. Geophys., 37, 275–316, 1999.

Solomon, S., Garcia, R. R., Rowland, F. S., and Wuebbles, D. J.: On the depletion of Antarctic ozone, Nature, 321, 895–899, 1986.

Solomon, S., Portmann, R. W., Sasaki, T., Hofmann, D. J., and Thompson, D. W. J.: Four decades of ozonesonde measurements over Antarctica, J. Geophys. Res., 110, D21311, doi:10.1029/2005JD005917, 2005.

Son, S. W., Gerber, E. P., Perlwitz, J., Polvani, L. M., Gillett, N. P., Seo, K. H., Eyring, V., Shepherd, T. G., Waugh, D., Akiyoshi, H., Austin, J., Baumgaertner, A., Bekki, S., Braesicke, P., Bruhl, C., Butchart, N., Chipperfield, M. P., Cugnet, D., Dameris, M.,

Dhomse, S., Frith, S., Garny, H., Garcia, R., Hardiman, S. C., Jockel, P., Lamarque, J. F., Mancini, E. Marchand, M., Michou, M., Nakamura, T., Morgenstern, O., Pitari, G., Plummer, D. A., Pyle, J., Rozanov, E., Scinocca, J. F., Shibata, K., Smale, D., Teyssedre, H., Tian, W., and Yamashita, Y.: Impact of stratospheric ozone on Southern Hemisphere circulation change: A multimodel assessment, J. Geophys. Res., 115, D00M07, doi:10.1029/2010JD014271, 2010.

SPARC CCMVal: SPARC report on the evaluation of chemistry-climate models, SPARC Rep. 5, edited by: Eyring, V., Shepherd, T. G., and Waugh, D. W., World Clim. Res. Programme, http://www.atmosp.physics.utoronto.ca/SPARC, 2010.

Stolarski, R. S. and Frith, S. M.: Search for evidence of trend slowdown in the long-term TOMS/SBUV total ozone data record: the importance of instrument drift uncertainty, Atmos. Chem. Phys., 6, 4057–4065, doi:10.5194/acp-6-4057-2006, 2006.

Thompson, D. W. J. and Solomon, S.: Interpretation of recent Southern Hemisphere climate change, Science, 296, 895–899, 2002.

Waugh, D. W. and Polvani, L. M.: Stratospheric Polar Vortices, The Stratosphere: Dynamics, Transport, and Chemistry, Geophys. Monogr. Ser., 190, 43–57, doi:10.1029/2009GM000887, 2010.

Waugh, D. W., Randel, W. J., Pawson, S., Newman, P. A., and Nash, E. R.: Persistence of the lower stratospheric polar vortices, J. Geophys. Res., 104, 27191–27201, 1999.

Waugh, D. W., Oman, L., Kawa, S. R., Stolarski, R. S., Pawson, S., Douglass, A. R., Newman, P. A., and Nielsen, J. E.: Impacts of climate change on stratospheric ozone recovery, Geophys. Res. Lett., 36, L03805, doi:10.1029/2008GL036223, 2009.

Wirth, V.: Quasi-stationary planetary waves in total ozone and their correlation with lower stratospheric temperature, J. Geophys. Res., 98, 8873–8882, 1993.

World Meteorological Organization (WMO) (2007): Scientific Assessment of Ozone Depletion: 2006, Rep. 50, Global Ozone Research and Monitoring Project, World Meterol. Organ., Geneva, Switzerland, 2007.